Low-Temperature FTIR Study of Multiple K Intermediates in the Photocycles of Bacteriorhodopsin and Xanthorhodopsin

ARTICLE *in* THE JOURNAL OF PHYSICAL CHEMISTRY B · FEBRUARY 2010

Impact Factor: 3.3 · DOI: 10.1021/jp908698f · Source: PubMed

3 AUTHORS, INCLUDING:

Andrei K Dioumaev
University of California, Irvine
38 PUBLICATIONS **1,127** CITATIONS
SEE PROFILE

Jennifer Wang
University of California, Irvine
25 PUBLICATIONS **741** CITATIONS
SEE PROFILE

Published in final edited form as:
J Phys Chem B. 2010 March 4; 114(8): 2920–2931. doi:10.1021/jp908698f.

Low-Temperature FTIR Study of Multiple K Intermediates in the Photocycles of Bacteriorhodopsin and Xanthorhodopsin

Andrei K. Dioumaev[*], **Jennifer M. Wang**, and **Janos K. Lanyi**
Department of Physiology & Biophysics, University of California, Irvine, CA 92697

Abstract

Low-temperature FTIR spectroscopy of bacteriorhodopsin and xanthorhodopsin was used to elucidate the number of K-like bathochromic states, their sequence, and their contributions to the photo-equilibrium mixtures created by illumination at 80-180K. We conclude that in bacteriorhodopsin the photocycle includes three distinct K-like states in the sequence:

$bR \xrightarrow{hv} I^* \rightarrow J \rightarrow K_0 \rightarrow K_E \rightarrow K_L \rightarrow L \rightarrow \ldots$, and similarly in xanthorhodopsin. K_0 is the main fraction in the mixture at 77K that is formed from J. K_0 becomes thermally unstable above ~50K in both proteins. At 77K both J-to-K_0 and K_0-to-K_E transitions occur and, contrarily to long-standing belief, cryogenic trapping at 77K does not produce a pure K state but a mixture of the two states, K_0 and K_E, with contributions from K_E of ~15% and ~10% in the two retinal-proteins, respectively. Raising the temperature leads to increasing conversion of K_0 to K_E, and the two states coexist (without contamination from non K-like states) in the 80-140K range in bacteriorhodopsin, and in the 80-190K range in xanthorhodopsin. Temperature perturbation experiments in these regions of coexistence revealed that in spite of the observation of apparently stable mixtures of K_0 and K_E, the two states are not in thermally-controlled equilibrium. The K_0-to-K_E transition is unidirectional, and the partial transformation to K_E is due to distributed kinetics, which governs the photocycle dynamics at temperatures below ~245K. From spectral deconvolution we conclude that the K_E state, which is increasingly present at higher temperatures, is the same intermediate that is detected by time-resolved FTIR prior to its decay, on a time-scale of hundreds nanoseconds at ambient temperature, into the K_L state. We were unable to trap the latter separately from K_E at low temperature, due to the slow distributed kinetics and the increasingly faster overlapping formation of L state. Formation of the two consecutive K-like states in both proteins is accompanied by distortion of *two different* weakly bound water molecules: one in K_0, the other in K_E. The first, well-documented in bacteriorhodopsin at 77K where K_0 dominates, was assigned to water 401 in bacteriorhodopsin. The other water molecule, whose participation has not been described previously, is disturbed on the next step of the photocycle, in K_E, in both proteins. In bacteriorhodopsin the most likely candidate is water 407. However, unlike bacteriorhodopsin, the crystal structure of xanthorhodopsin lacks homologous weakly-bound water molecules.

Keywords

hydrogen out of plane (HOOP) vibrations; bathointermediates; distributed kinetics; retinal-proteins; *Halobacterium salinarium*; *Salinibacter rubber*

[*]To whom correspondence should be addressed. Voice phone (949) 824-7783; FAX (949) 824-8540; dioumaev@uci.edu.

Introduction

Retinal-proteins constitute a rapidly expanding family[1-4] of mostly microbial proteins that can use light for either energy (pumps)[5] or signaling (sensors)[6]. Upon absorption of quanta in the visible region, they undergo a cycle of internal transformations that include several obligatory steps. Using the notation H to O to describe the consecutive intermediates first introduced for bacteriorhodopsin[7,8], these steps include: (i) the initial photophysics (the excited states of H*, I*) where the energy of the absorbed quantum is within the chromophore; (ii) the primary photochemistry (the J, and the K-like states) when the retinal is isomerized and the protein begins to readjust to accommodate the new chromophore configuration as the energy is transferred from the chromophore into its immediate environment, and (iii) further steps in which the excess energy stored in the chromophore is fully transferred into the protein. The last phase will depend on the specific function of the protein, but the first two seem to be of general validity, and the sequence of the K-like states covers an important stage in the energetics of the photochemical cycle.

The red-shifted primary intermediates are a general feature in the light-induced photocycles of retinal-proteins. In bacteriorhodopsin, as earlier in the visual pigment, a bathochromic state was trapped at 77K[9,10], and called K according to the notation proposed in[7]. When its predecessor was discovered by picosecond spectroscopy[11], it was called J[8]. Unlike K, the J state cannot be trapped even at 77K[12]. In the visible region, both J and K states are bathochromic, J being more strongly red-shifted than K[11,13].

The K state(s) is not a single intermediate[14-16] but rather a generic term for a sequence of spectrally-similar species, which at room temperature span the time-domain from ~10^{-11} to ~10^{-6} seconds. The existence of more than one K-like intermediate is supported by evidence from the variety of experimental methods: in visible[14,16-20], UV[21], and FTIR spectroscopy[15,22-28], resonance Raman[29-31], CARS[32], and photoelectric measurements[33]. The necessity for more than one K-like intermediates has been evident since early eighties[14,15] but the question on their number has not been settled, and most authors restrict their discussions to the possibility of *two* different K-like states[14-18,21-31]. However, two K-like states are not enough to account for the changes during the early stages of the photocycle, and the pair of K-like intermediates described by time-resolved[24-28] FTIR spectroscopy cannot be the same as the pair of intermediates characterized by low-temperature FTIR[15,34]. Instead, the similarities in the IR spectra between the "high-temperature" state[15], i.e. the "later" one of the two K states revealed by cryogenic trapping, and the "early K" state[28] described by time-resolved data indicate that *three* different K-like intermediates appear in sequence in the bacteriorhodopsin photocycle between the J and the L intermediates.

The vibrational spectra of the K-like state(s) have been studied in detail, by resonance Raman[29,30,35-39], CARS[32,40], and IR methods[15,23,41-45], using static (i.e. trapped at cryogenic temperature)[15,35,41-44,46-48] and time-resolved[23-30,36-40,45] techniques. Detailed assignment of individual vibrational modes was through extensive use of isotope-labeled retinal incorporated into bacteriorhodopsin by Raman[49] (and most fully summarized in[50]) and by FTIR[44,46,51] methods, creating the basis for studies of other retinal-proteins. Both in bacteriorhodopsin[35,41,42] and the other microbial rhodopsins[52-60] the spectra revealed a well-defined pattern of intensities in the region of hydrogen-out-of-plane (HOOP) vibrations. The HOOP bands are typical for the K-like states, as the other intermediates in the photocycle, with a notable exception of the O state[61], give rise to little if any intensity in this region[62]. This makes them a convenient feature for monitoring K-like states in microbial rhodopsins. While the early bathochromic intermediates are common to all microbial rhodopsins, their spectra, and especially the pattern of their HOOP bands vary

strongly[52-60]. It was proposed that retinal-proteins with sensor and pump function could be distinguished by their HOOP band patterns[63]. We argue here that at least part of the variability in the HOOP of different retinal-proteins[52-60] is due to the presence of multiple different K intermediates.

We find that the IR spectra of the K-like states in xanthorhodopsin (a proton-pumping retinal-protein/carotenoid complex from *Salinibacter ruber*[64]) is surprisingly similar to those in bacteriorhodopsin, much more so than for other microbial rhodopsins[52-60]. Specifically, the HOOP region, where the temperature-dependent differences between different K-like states were initially found[15], is very similar in the two proteins. However, unlike in bacteriorhodopsin where L formation interferes with monitoring of K above ~140K[48], in xanthorhodopsin the temperature region where only K-like states are present is extended to ~190K. This allows a greater extent of temperature-induced transformation and thereby facilitates spectral deconvolution. We found that the interconversions between K-like states is governed by distributed kinetics, which effectively inhibits complete conversions between the states[48,65], and the extended temperature range in xanthorhodopsin created an opportunity, which we exploited for studying the multiple K-like states.

Experimental Methods

Purple membranes containing wild-type bacteriorhodopsin were isolated according to a standard procedure[66]. Membrane fraction of xanthorhodopsin was isolated as in[64,67]. The samples used were at pH 7.0 and 8-8.5 (1 mM HEPES buffer) for bacteriorhodopsin and xanthorhodopsin, respectively.

Sample preparations and FTIR measurements were as described previously[48,65,68]. In short, infrared measurements were performed at 2 cm^{-1} resolution on Bruker IFS-66/s Fourier-transform infrared (FTIR) spectrometer on humidified films of the membrane fragments of xanthorhodopsin and bacteriorhodopsin containing >600 water molecules per molecule of the protein[68]. Low temperature was provided by the Optistat DM cryostat equipped with the ITC601 temperature controller (both from Oxford Instruments, Abingdon, UK). Temperature equilibration required ~80 minutes, after which the cryostat system provided temperature stability within 0.1 K for >5 hours. Prior to any measurements, the samples were light-adapted at 280K for 20 min with a lamp equipped with a 500±20 nm interference filter (referred to as “blue light”). Spectra of intermediates were measured as differences in the IR absorption before and after illumination with blue light, co-adding of 1119 interferograms for each spectrum during a 10 min data collection time. Between any pair (of measurements, before and after illumination) the sample temperature was raised to 280K to complete the photocycle and restore the initial state.

The spectra were interactively corrected for water vapor and, where needed, for base-line distortions. For comparison of spectra measured in separate experiments, the bacteriorhodopsin and xanthorhodopsin spectra were normalized at 1254 and 1253 cm^{-1}, respectively. When a series of spectra trapped at different temperatures required simultaneous analysis, singular value decomposition (SVD) was used. SVD, a matrix algorithm, allows separation of systematic features form stochastic noise[69], and effectively averages the spectral data over all measured spectra. It improves, therefore, the extraction of spectra of the pure forms from their mixtures.

While IR spectroscopy allows direct monitoring of the overall amount of water in the sample containing retinal-proteins[68], it is not capable of monitoring the distribution of water molecules throughout the sample. Humidity does affect the mixtures trapped at cryogenic temperatures. The main effect observed in the IR is from the contaminating presence of the

13-*cis*,15-*syn* retinal in non-excited samples (data not shown), which in is due to incomplete light-adaptation under low humidity[70]. The latter gives rise to a red-shifted photoproduct, different from the K-like states produced from all-trans retinal, and in IR the most affected bands are in the amide, ethylenic stretch, and finger print regions[71,72]. No HOOP bands are seen upon light-adaptation[42,71] but there are conflicting reports on whether the HOOP bands are present in the low-temperature photoproduct(s) of the 13-*cis*,15-*syn* retinal at 77K[71,72]. Our measurements on bacteriorhodopsin samples of different humidity in the 80-140K range produced spectra, which do differ in the ethylenic and finger print regions, reflecting incomplete light-adaptation and participation of the 13-*cis*,15-*syn* chromophore. However, the presence of the photoproduct(s) of the 13-*cis*,15-*syn* retinal fails, in accord with the 77K data of the Rothschild group[71], to affect the HOOP region (our unpublished data). Since the conclusions in this paper are primarily based on the analysis of the HOOP band region, we believe that they are, therefore, free from the potentially disturbing influence of limited hydration and potentially incomplete light-adaptation.

OPUS (Bruker, Germany), *GRAMS* (Galactic Industries Corp., Salem, NH), *Matlab* (The MathWorks Inc., Natick, MA), and *KaleidaGraph* (Synergy Software, Reading, PA) software were used for data evaluation and presentation.

Results

IR spectra obtained at 80K after 10 min illumination with blue light (500±20 nm) of bacteriorhodopsin and xanthorhodopsin films equilibrated with H_2O and D_2O are presented in Figure 1A and 1B, respectively. The spectra in Figure 1A are the well-described low-temperature K spectra of bacteriorhodopsin[41-43]. The similarity between the spectra of bacteriorhodopsin (Figure 1A) and xanthorhodopsin (Figure 1B), and specifically the pattern of the HOOP bands (Figures 2B and 2D), is extraordinary, and the xanthorhodopsin spectra are more like those of bacteriorhodopsin than most of other retinal proteins, e.g., halorhodopsin[52], pharaonis[53,54,59] and Anabena[57] sensory rhodopsins, proteorhodopsin[55,60], Neurospora rhodopsin[56,58], and Leptosphaerium rhodopsin[58].

Besides the similarity of the K spectra in the two proteins (Figures 1A and 1 B), there are distinct differences as well. The first is the higher amplitudes and more structured pattern of the majority of the bands in the 1200-1500 cm^{-1} region, relative to the strongest bands of the difference spectrum in the ethylenic, finger-print and HOOP regions. This could be partly due to anisotropy/polarization effects[73,74] but our main impression is that the spectrum of xanthorhodopsin at 80K (Figure 1B) reflects much stronger and more numerous bond distortions than the respective spectrum in bacteriorhodopsin (Figure 1A). Detailed studies of this is not possible at this stage because of lack of an expression system for constructing mutants of xanthorhodopsin, but the possibilities include contributions from the carotenoid, salinixanthin, which acts as an antenna for retinal in xanthorhodopsin[64]. The carotenoid is expected to be disturbed during the early stages of the photocycle, and, if so, will give rise to bands very similar to those of the retinal. The second difference is in the C=O stretch region: the bilobe feature at 1731/1739 cm^{-1}, which reflects a distortion in the carboxyl COO^- stretch vibration that results in the up-shift of the corresponding band. Most probably, it is due to either a decrease in the hydrogen-bonding strength, or to a transiently increased proton affinity of the COOH group[75]. In bacteriorhodopsin, a similar but lower amplitude bilobe feature at 1730/1740 reflects an opposite change that leads to the down-shift of the $COOH^-$ stretch band. The third difference is the anomalous D_2O-sensitive behavior of the 1253 cm^{-1} band in xanthorhodopsin, unexpected because it is normally attributed to the C_{12}-C_{13} vibration of the retinal[50]. The fourth difference consists of the D_2O-enhanced bands in the 1010-1110 cm^{-1} region, which have never been properly assigned.

Raising the temperature from ~80K to 135K gives rise to partial conversion from the low-temperature to a higher-temperature K intermediate, which strongly affects the HOOP band region[15]. This process is even more pronounced in xanthorhodopsin, in which, unlike in bacteriorhodopsin[48], the rise of L does not interfere with the K spectra until above 190K. Figure 2 presents the spectra of photo-equilibrium mixtures created by blue-light illumination at different temperatures. The spectra of bacteriorhodopsin and xanthorhodopsin retain their similarity with increasing temperature (Figures 2 and 3), indicating that a similar secondary K-like intermediate is produced in both proteins upon heating (Figures 2B and 2D). The greatest changes between the two K-like intermediates are in the HOOP region, which is shown in more detail in Figures 2B and 2D. Other strong changes (Figures 2A and 2C) affect the amplitudes of the following features: (i) in the carboxylic region the up-shift from 1731 to 1739 cm^{-1} in xanthorhodopsin and the downshift from 1739 to 1730 cm^{-1} in bacteriorhodopsin; (ii) the protonated Schiff base stretch, which is at 1608-1609 cm^{-1} in bacteriorhodopsin[50,51], and we tentatively assign the analogous band at 1611 cm^{-1} in xanthorhodopsin to the same mode; (iii) the ethylenic band at 1514 in bacteriorhodopsin and at 1511 cm^{-1} in xanthorhodopsin; and (iv) the fingerprint region band at 1194 cm^{-1}. Other notable changes in the two proteins are in the two amide regions: near 1660-1700 and 1560-1580 cm^{-1}. Bands at 1353 cm^{-1} and 1389 cm^{-1} in bacteriorhodopsin and xanthorhodopsin, respectively which are most probably due to the N-H wag[50], disappear with increasing temperature.

The extended temperature range for xanthorhodopsin where K is the sole product reveals details not immediately evident in bacteriorhodopsin spectra. Specifically, at 190K the pattern of the HOOP bands (Figure 2D) becomes virtually indistinguishable from that of the K_E intermediate (see Figure 4 in[28]), the first of the two K states time-resolved in hundreds of nanoseconds at room temperature. This is not immediate evident in the data for bacteriorhodopsin but is revealed by spectral deconvolution (see below). The agreement of the spectra establishes a correlation between the second K-like state observed here at higher temperature in cryogenic trapping and the time-resolved K_E state observed at room temperature.

Spectral decomposition, performed with the *GRAMS* software, revealed that the HOOP band region is a superposition of six separate positive bands. These are at 942, 956, 963, 975, 985, and 997 cm^{-1} in bacteriorhodopsin, and at 942, 954, 960, 971, 981, and 992 cm^{-1} in xanthorhodopsin, respectively. Figure 3 illustrates this deconvolution for spectra measured in both bacteriorhodopsin and xanthorhodopsin. Figure 4 presents the temperature dependence of the fitted amplitudes for the six HOOP bands in xanthorhodopsin (the analogous data for bacteriorhodopsin are not shown). Only two bands, at 960 and 981 cm^{-1}, are strongly temperature sensitive (Figure 4), and the pattern of their temperature dependence suggests the possibility of a temperature-controlled equilibrium between two K-like intermediates.

To test this option, we performed temperature-jump experiments, in which the photo-equilibrium created at 80K was heated to 140K for measurements, and the one created at 140K was cooled to 80K for measurements. The result is presented in Figure 5, from which it is evident, that *up-shift* of temperature does lead to the expected shift in the mixture composition while *down-shift* fails to affect the composition of the mixture. Thus, the temperature perturbation experiment reveals the absence of the back-reaction, and what looks like an apparent balance in Figure 4 cannot originate from a temperature-controlled equilibrium. The remaining alternative is the distributed kinetics we had found earlier, with a similar approach, for other transitions in bacteriorhodopsin at temperatures below ~245K[48,65].

That distributed kinetics describes the low-temperature transformations between the K-likes states is not a surprise *per se*, since it was observed for both L formation[48] and L decay[65] at still higher temperatures. However, for the L transitions not only the partial transformation but the characteristic time-progression of the distributed kinetics could be observed in real time[48,65]. Here, we were not able to time-resolve the transformation between the K intermediates. It appears that at all temperatures the apparent partial transformation (Figure 4) was accomplished within the illumination period (1-10 min), and the created photo-induced mixture was then stable on the time-scale of several hours. This behavior implies that, unlike for the next, K-to-L, transition (for which the underlying barrier-height distribution has a half-maximal width of ~7 kJ/mol[48]), the energy barriers distribution for transitions between K-like states must be wide, allowing substantial transformations both on the fast (< 1 min) and extremely slow (> 200 min) time-scales.

The temperature-controlled redistribution pattern of HOOP intensities (Figures 2, 3, and 4) indicates that the large 981 cm^{-1} band (in xanthorhodopsin and at 985 cm^{-1} in bacteriorhodopsin) is specific to the K-like state that dominates at higher temperatures. It is produced from the previous K state at lower temperature (Figure 5A), for which the HOOP band at 961 cm^{-1} (in xanthorhodopsin and at 956 cm^{-1} in bacteriorhodopsin) is specific. The temperature dependence (Figure 4 for xanthorhodopsin; analogous data for bacteriorhodopsin are not shown) indicates that neither of the two intermediates is trapped in pure form throughout the entire 80-180K range, but both are present as temperature- and protein-specific mixtures. This is true even at 77K, a temperature at which the trapping is widely assumed to produce a single K state.

To obtain the pure spectra of the two K intermediates, the spectra (for bacteriorhodopsin and xanthorhodopsin in Figures 2A and 2C, respectively) were at first subjected to singular value decomposition (SVD). SVD produced in both cases two statistically significant spectral components, reflecting a presence of two spectrally-distinct intermediates. Since the K spectra have many common features (see Figure 2), the first SVD component is effectively a (weighted) sum of the spectra of the two intermediates, while the second component is their difference; both are averaged over all temperatures. A weighted (with singular values) sum and difference of the first two SVD components, an orthogonal pair of abstract spectra, were constructed, which represent a starting estimate for the pure spectra of intermediates. These spectra were then rotated, without compromising their orthonormality, with the aim to obtain simultaneously in the *first* spectrum maximum amplitude for the ~960 cm^{-1} band *and* as little as possible (but non-negative) absorption at ~980 cm^{-1}. This rotation creates the spectrum of the state dominating at low temperatures but already lacking the contribution of the higher-temperature state. Since the real spectra are not orthonormal, the initial rotation leaves significant contribution of the K intermediate that dominates at low temperature, in the *second* spectrum. The latter was eliminated by interactive subtraction. The two calculated spectra were normalized (at 1254 for Figure 6A or 1253 cm^{-1} for Figure 6B), and the result, the spectra that would have been measured for the two pure K-like states in bacteriorhodopsin and in xanthorhodopsin are presented in Figure 6.

Once the measured spectra (in Figure 2) were decomposed into two pure components (in Figure 6), their related contributions, as a function of temperature, could be calculated. In matrix notation, the spectra (in Figure 2) measured at different temperatures, $\|\Delta A(v, T)\|$, could be represented as a product of pure spectra of the respective states, $\|spectra(v,i)\|$, and their temperature-dependent (partial) contributions, $\|contributions(i,T)\|$:

$$\| \Delta A(v,T) \| = \| spectra(v,i) \| \cdot \| contributions(i,T) \| . \quad (1)$$

Therefore, a least-square estimate (averaged over the whole spectrum) for related contributions is readily obtained using the matrix pseudoinverse function[69]:

$$\| \, contributions\,(i,T) \, \| = \mathrm{pinv}\,(\| \, spectra\,(v,i) \, \|) \cdot \| \, \Delta A\,(v,T) \, \|, \quad (2)$$

where pinv(||*spectra(v,i)*||) = (||*spectra(v,i)*||$^{\mathrm{T}}$·||*spectra(v,i)*||)$^{-1}$·||*spectra(v,i)*||$^{\mathrm{T}}$, and || ||$^{\mathrm{T}}$ and ( )$^{-1}$ are the matrix transpose and matrix inverse, respectively. The result is shown in Figure 7. When compared in the same temperature region (80-140K), the temperature dependences for the composition of the mixtures that are trapped at different temperature are very similar in both proteins. Extrapolation of these temperature dependences in Figure 7 predicts that the two K intermediates should be expected to co-exist in the temperature range from ~50 to ~230K. This estimate is true for both bacteriorhodopsin and xanthorhodopsin, but this range might differ in other proteins. For example, while it takes temperatures >80K to observe this transition in both (wild-type) bacteriorhodopsin and xanthorhodopsin, it seems to be nearly completed already at 77K in Leptosphaerium rhodopsin[58] and in the Y57D mutant of bacteriorhodopsin (see Figure 5 in[76]) and probably in Salinibacter sensory rhodopsin I (see Figure 2 in[63]) as well.

The strongest differences between the two K states, in the HOOP region, are evident already in the raw data (Figures 2B and 2D); other differences were revealed by the spectral decomposition (Figure 6). These differences are similar in the two proteins, but most seem more pronounced in xanthorhodopsin. A characteristic change is in the carboxylic region, where a down-shift and an up-shift of the carbonyl band are present in the low-temperature spectra of bacteriorhodopsin and xanthorhodopsin, respectively (Figures 1 and 6). In xanthorhodopsin the transition from the low-temperature to the higher-temperature K state affects the bilobe difference carbonyl band at 1739/1730 cm^{-1}, which loses some of the negative (depletion) amplitude without a comparable effect on the positive amplitude. In bacteriorhodopsin the effect is the opposite, and it is the positive amplitude of the bilobe feature at 1739/1730 cm^{-1}, which seems to be primarily affected. Most probably the same explanation applies to both: a second carboxylic acid additionally disturbed in the species that dominates at higher temperatures; although, xanthorhodopsin lack a homologue of Asp-115 in bacteriorhodopsin. In both proteins the protonated Schiff base stretch, at 1608 cm^{-1} in bacteriorhodopsin[42,51] and at 1611 cm^{-1} in xanthorhodopsin, are up-shifted to 1625 and 1619 cm^{-1}, respectively. The ethylenic band, at 1514 cm^{-1} in bacteriorhodopsin and 1511 cm^{-1} in xanthorhodopsin, is not significantly affected, implying the absence of a substantial (>5 nm) difference in the visible absorption maxima of the two K intermediates. The depletion band at 1389 cm^{-1} disappears in both proteins at higher-temperatures, as a result appearance of an overlapping positive band (at 1397 cm^{-1} in both bacteriorhodopsin and xanthorhodopsin). This band is most probably due to in-plane methyl rock, which spans the 1270-1360 cm^{-1} range in bacteriorhodopsin[50], or it could reflect the symmetric band of a deprotonated carboxylic acid[77]. An analogous effect is observed in xanthorhodopsin at 1239/1247 cm^{-1} (Figure 6B). The corresponding band is most probably from protonated tyrosine[77]. In bacteriorhodopsin this effect is much less pronounced but the change in the absorption in the 1210-1250 region is obvious (Figure 6A).

While the differences between the two K-like states observed at cryogenic temperatures is spread thought the whole mid-IR region (Figure 6), the most characteristic changes are in the HOOP region, and the latter primarily influence the calculated ratios of the partial contributions. The ratios (Figure 7) are sensitive to potential errors in spectral deconvolution (in Figure 6), and the strong dependence on one particular feature, the HOOP bands, makes them somewhat unreliable. Therefore, we looked for independent evidence outside the mid-IR region, and explored the O-H stretch region of the free, or weakly hydrogen-bonded water (>3600 cm^{-1}) in which differences was previously found between the K-like states

trapped at 77K[78], and at 135K[34]. Figures 8A and 8C presents the measured data that reflects characteristic change in the O-H stretch region in bacteriorhodopsin and xanthorhodopsin, respectively, which is dominated by contributions from one[34] or two (as we think more likely) different weakly hydrogen-bonded water molecules. As was reported earlier[78], the main feature in the mixture at 80K is the down-shift of the 3644 cm^{-1} (3649 cm^{-1} in xanthorhodopsin) band to 3637 cm^{-1}, originating from an increased interaction of a water molecule, observed already at the lowest temperature (~80K). These bands are shifted in D_2O and in $H_2{}^{18}O$[34,78], and disappear in Y57D mutant[78]. The depletion band at ~3644 cm^{-1} is also present in both L[78,79] and M states[78].

In contrast, the main apparent feature in the mixture at 140K seems to be the up-shift of a band to ~3653 cm^{-1} (in bacteriorhodopsin, and to ~3657 cm^{-1} in xanthorhodopsin), originating from a decreased interaction of either the same water[34] or an O-H stretch, different from that of the water molecule affected at 80K.

It is important that in addition to these dominant features at the two extreme temperatures, each of the spectra at 80 and 140K (Figures 8A and 8C, as well as the other spectra shown for bacteriorhodopsin in the 80-140K range in Figure 8A) contain weaker additional bands at ~3637 cm^{-1} at 80K and the 3644-3649 cm^{-1} band at 140K. The simultaneous presence of these distortions at both 80 and 140K could be rationalized by temperature-induced conversion from one state into the other. If the states trapped at both low (at ~80K) and high (at ~140K) temperatures are (almost) pure states, as was assumed in[34], the single depletion band at 3644-3649 cm^{-1} (Figures 8A and 8C) originates from a single water molecule, and it is the mode of its distortion that is changed upon the temperature-induced conversion from one state into the other. Alternatively, the spectra at the low and high temperatures represent mixtures of two K intermediates, as suggested by our treatment of spectra in the mid-IR region (Figures 6 and 7), and, therefore, the change in spectra is due to partial redistribution between those states (at 80 vs. at 140K) that are not present in pure form at either temperature. If there are mixtures of the two states at all temperatures, as we argue, these two states could involve participation of different water molecules, specifically perturbed in one but not in the other state.

To test the spectral deconvolution in Figure 6, we used the partial concentrations calculated from the mid-IR region (Figure 7) to decompose measured spectra in the water region (in Figures 8A and 8C) into two components, which would reflect the pure spectra of the two K states dominating at low- and high temperature, respectively:

$$\| \, spectra\,(v,i) \, \| = \| \, \Delta A\,(v,T) \, \| \cdot \mathrm{pinv}\,(\| \, contributions\,(i,T) \, \|) \quad (3)$$

The results are shown in dashed lines in Figures 8B and 8D for bacteriorhodopsin and xanthorhodopsin, respectively. Two important features become evident from such deconvolution. The first is that, unlike the raw data (Figures 8A and 8C) the recalculated spectra (of what we expect to be almost pure states at low and higher temperatures, respectfully) strongly indicate the presence of two distinct depletion bands at 3644/3649 and 3635/3636 cm^{-1} (in bacteriorhodopsin and xanthorhodopsin, respectively). The second feature is that both extrapolated spectra still seem to be partly contaminated by the spectrum of the other state. To estimate the magnitude of this cross-contamination, we interactively subtracted these spectra (dashed lines in Figures 8A and 8C) from one another with the target to further separate the two tentative depletion bands. The result of this subtraction is shown as solid lines in Figures 8B and 8D for bacteriorhodopsin and xanthorhodopsin, respectively. To test the validity of this adjustment, the fractional concentrations were then recalculated using Eq. 2, now based on the spectra (solid lines in Figure 8B and 8D) from the water-region deconvolution. The fractional concentrations (as in Figure 7) were similar

to those from the HOOP deconvolution. In xanthorhodopsin the strongest change is in the calculated fractions at the highest end of temperature data: the mixture composition at 180K is changed from ~30:70 to ~40:60. In bacteriorhodopsin the effect is on the lowest end of the temperature range, and the corresponding ratios in the mixture composition are changed from ~80:20 to 85:15. We believe that these differences are within the limit of accuracy of our method, and the separation of the two water bands, with little contamination of one with the other, goes hand-in-hand with the HOOP band separation. Thus, the spectra from the water region confirm that the two K intermediates are trapped as mixtures at both 80 and 140K.

Separation of the contribution of the two K intermediates in the mixtures trapped at different temperatures resulted in two distinct depletion bands in the water region of both proteins (solid lines in Figures 8B and 8D), indicating involvement of two different weakly hydrogen-bonded water molecules in the K states. This conclusion is in contradiction with the interpretation in[34]. Further, each of the two disturbed waters is specific for one of the two K-like states trapped. In both proteins the water (Figures 8B and 8D), which has a depletion band (i.e., absorbs in the non-excited state) at 3644 and 3649 cm^{-1} (in bacteriorhodopsin and xanthorhodopsin, respectively), is the only water disturbed in the K-like state predominant at lower temperatures. The pattern of the distortion of the other water molecule in the two proteins was found to be different (Figures 8B and 8D) from what it might have looked like in the measured spectra (in Figures 8A and 8C): its depletion band (i.e., the band of non-excited bacteriorhodopsin and xanthorhodopsin) is some 10-15 cm^{-1} below the position of the apparent minimum (in Figures 8A and 8C) and is at 3636/3635 cm^{-1}. This band is present only in the higher temperature K state, which constitutes ~50% of the mixture at ~140K in both proteins, and upon its formation the band is up-shifted to 3653 cm^{-1}.

The apparent depletion band at ~3645 cm^{-1} (first observed in bacteriorhodopsin[78]) was at first tentatively assigned to a water molecule close to Tyr-57[78] and later to water 401[34] in the crystal structure of bacteriorhodopsin[80]. This high frequency implies that it originates from a non hydrogen-bonded, or weakly hydrogen-bonded O-H[81]. If there are two distinct although not greatly different depletion bands, as we observe (Figure 8B), the assignment would have to include water 407 as well, the other water molecule in the vicinity of the Schiff base which also has a non hydrogen-bonded O-H group and could have an O-H stretch above 3600 cm^{-1}.

In xanthorhodopsin, interpretation of the directly observable depletion band (Figure 8C) in the region of very weakly bound water is much less clear. The crystallographic structure[67] reveals only three water molecules, and only one of them, water-402, in the extracellular region vs. seven in bacteriorhodopsin[80]. This is not likely to be an artifact because the hydrogen-bonds that involve water in bacteriorhodopsin are present in xanthorhodopsin also, but they are to main-chain atoms[67]. Water-402 in xanthorodopsin[67] is the analogue of water-402 in bacteriorhodopsin[80], and, therefore, is a poor candidate for a non hydrogen-bonded O-H stretch[67,80]. The paucity of other water molecules makes the assignment of the second depletion band in this region, at 3635 cm^{-1}, problematic. This band has to be from a non hydrogen-bonded O-H stretch[81]. Besides water, –OH groups are in Ser, Thr, Tyr, as well as Asp and Glu, but these seem to be ruled out by the fact that the bands are shifted by $H_2{}^{18}O$ exchange[34,78].

Discussion

As discussed in the Introduction, the need for more than one K intermediate has been recognized for a long time, but the usual option was a second K-like state when one was not

sufficient to account for the data[14-31]. The only evidence for more than two distinctly different K states was in[19], where the interpretation focused on conformers formed in parallel from an inhomogeneous population of bacteriorhodopsin at cryogenic temperatures. Here we report on multiple distinct K intermediates. Unlike the three K states in[19] (see also[34]) that differed in their convertibility by visible light of different wavelengths, the two K-like states here (Figure 6) exhibit little if any shift in the ethylenic band, and therefore are expected[82] to have the same visible absorption maximum.

These two K intermediates are formed in sequence in the main path of the photocycle. We do observe them at low temperatures but neither their number nor their sequence is restricted to cryogenic temperatures, and they can be observed at room temperature as well. The two modes of studying the photocycle, low-temperature trapping and time-resolved monitoring, produce complementary results. However, the spectral changes measured reflect complex mixtures rather than pure intermediates in both time-resolved[83-85] and cryogenic trapping[48,62,65] data. Their quantitative comparison is made difficult by the complexity of the deconvolution[83,84,86], and at least part of the well-documented discrepancies (see for example[24,84]) could be due to incomplete separation of the intermediates involved. We believe that multiple distinct K intermediates reported here and previously[16,28] would help to reconcile some of the conflicting data on the early stages of the photocycle.

Interconversions between the K intermediates lead to characteristic changes in the HOOP region (Figures 2B and 2D), and these states co-exist free from contamination from non K-like states (Figures 2A and 2C) in a wide temperature rage. In bacteriorhodopsin this range spans ~60K, between 77 and ~140K. In xanthorhodopsin the temperature-induced variations in spectra are very similar to that in bacteriorhodopsin (Figures 2A and 2C), and their HOOP regions are practically indistinguishable (when compared in the same temperature region, Figures 2B and 2D) but the region of co-existence of the two K states uncontaminated by other states (Figure 2B) is increased to span ~110K, between 77K and ~190K (Figure 2C).

It was this extended temperature range in xanthorhodopsin (Figures 2C and 2D), which enabled a more complete conversion and facilitated deconvolution of the two low-temperature K-like states (Figures 3, 4 and 6). The IR spectra (Figure 6B), especially their HOOP region, allowed us to conclude that the K state that dominates at higher temperatures is equivalent to K_E, the *first* of the two K-like states, which were detected in time-resolved measurements at room temperature[28]. Thus, the combination of static low-temperature[15,34] and time-resolved ambient-temperature[24-28] IR spectra provided the initial evidence, but the data from xanthorhodopsin (Figure 6B) and its comparison with the time-resolved spectra[28] and static spectra from bacteriorhodopsin (Figure 6A), has lead to the unambiguous conclusion that there are three distinctly different K intermediates, and they occur in sequence in the photocycles of the two proteins.

Therefore, based on the results in this paper, and supported by a large body of consistent evidence in the literature (see Introduction), we believe that the initial part of the photocycle is described by the following sequence:

$$bR \xrightarrow{h\nu} I^* \rightarrow J \xrightarrow{<4K} K_0 \xrightarrow{\sim 50K} K_E \xrightarrow{??} K_L \xrightarrow{\geq 140K} L \xrightarrow{\geq 175K} \ldots \quad (4)$$

where the numbers above the arrows indicate the threshold temperatures, i.e. the stability region for the previous intermediate (for bacteriorhodopsin). A similar sequence of K states occurs in the xanthorhodopsin photocycle. The first state that we propose to call K_0, is preferentially trapped at 77-80K[41-43] and while it is routinely considered to be the only contribution at this temperature, our estimate is that it accounts for ~85% of K at 77K. The second one, K_E, was first noted in the mixture trapped at 135K[15], in which according to our

estimate it accounts for ~50% of K. K_E is observed as a dominant contribution in room-temperature time-resolved experiments at ~100 ns after excitation[28]. K_L, which is the product of the K_E decay[28] at ambient conditions, cannot be trapped separately from K_E at cryogenic temperatures, due to the slow distributed kinetics and the increasingly faster overlapping formation of L[48].

In bacteriorhodopsin at ambient conditions the time constant of J state formation is 430±50 fs[87]; that of the first of the K-like states, K_0, is ~3-5 picoseconds[13,88]. The last of the K states, K_L, decays into L with a time constant of ~ 1.2 μs[83]. Two additional transitions were reported within the life-time of the K-like states with the time constants of (i) 30-70 ps[23,31,38], and (ii) 50-250 ns[16,28,32], respectively. We assign the former, with the τ_1=50±20 ps time constant, to the K_0-to-K_E transition; the latter, with the τ_2=150±100 ns time constant, had been already assigned to K_E-to-K_L transition[16,28].

The transition from K_0 to K_E results in pronounced rearrangement of bands in the HOOP region. In the K_0 state the strongest band is at ~956 cm^{-1} (961 cm^{-1} in xanthorhodopsin), which is readily observed when measured either by trapping below ~90K (Figure 1 and[41,42]) or with a picosecond time-resolution[39]. In the K_E state the strongest band is at ~985 cm^{-1} (Figures 2, 3 and 6), and it is observed in bacteriorhodopsin either as a partial component in a mixture when trapped at 135K (see Figure 2B and[15,34]), or in a nearly pure form when measured with nanosecond time-delay[28,89]. Unlike in bacteriorhodopsin where L formation interferes, in xanthorhodopsin K_E becomes the major component when trapped at 170-190K (Figures 2, 3, 4, and 6). Further changes in the HOOP region, which are observed in the ~50 ns to ~5 μs range[24-28], indicate the next process, the decay of K_E into K_L. Unlike the previous transitions, the latter process does not lead to a significant change in the pattern of HOOP band, but rather leads to an overall decrease of their amplitude in K_L[28]. Otherwise, K_L has a spectrum[28] that is quite different, particularly in the ethylenic stretch region, from the two previous K-like states, K_0[15,41-43] or K_E[15,28]. Therefore, contrarily to the conclusions in[34] (see also[58]), K_L has little to do with the observed changes between the mixtures trapped at ~80K and at ~135K[15,34]. Unlike the K-like states, their predecessor, the J state, has either much smaller or no HOOP bands at all[39], and is not trappable at cryogenic temperatures[12].

The HOOP bands originate from the wags of the vinyl protons in retinal, from vibrations which are strongly coupled over the double bonds and weakly coupled over the single bonds[90]. There is general agreement that anomalously intense HOOP bands observed in the primary bathoproducts (i.e., K-like states) indicate an unrelaxed torsion distortion of the polyene chain[90,91], since retinal in solution is planar and does not give rise to HOOP bands (in Raman)[91]. There is less agreement about which single or double bonds in the conjugated backbone are distorted and are, therefore, primarily responsible for the HOOP band intensities. The HOOP bands were attributed both to the single bond distortions[24,91,92], i.e. to wags of $C_{10}H$-$C_{11}H$ with coupling to $C_{12}H$, and of $C_{14}H$-$C_{15}H$ with coupling to NH, and to torsion distortions of double bonds[90,93], i.e. to C_7H=C_8H, $C_{11}H$=$C_{12}H$, and $C_{15}H$=NH.

The main assignments of the HOOP bands in the microbial rhodopsins were made by Raman spectroscopy for the K state of bacteriorhodopsin, which at 5 cm^{-1} resolution[35] detected four bands[36,50] relevant to our study, at 943, 958, and 975 plus at 1348 cm^{-1}. The 975 cm^{-1} band was assigned to the wags of the C_7-H and the C_8-H (i.e., coupled in-phase vibrations of the vinyl protons in $-HC_7$=C_8H); the 943 cm band to the wags of $C_{11}H$ and C_{12}-H (coupled in-phase in $-HC_{11}$=$C_{12}H$-), while the 958 cm band to the isolated wag of C_{15}-H coupled to the N-H wag at 1348 cm^{-1}. The corresponding out-of-phase vibrations are at 823 and 868 cm^{-1} for the C_7-H/C_8-H and C_{11}-H/C_{12}-H, while the bands for the C_{14}-H and C_{10}-H wags, which are separated from a neighboring C-H by an uncoupling single bond, are at 812 and 899 cm^{-1}, respectively, i.e. all below 900 cm^{-1} (see more in[50]).

Thus, in the crucial region of 945-995 cm^{-1} Raman assignments are available for only three bands, at 943, 958, and 975 cm^{-1}, while deconvolution of the IR data produces six positive bands for K-like states: at 942, 956, 963, 975, 985, and 997 in bacteriorhodopsin (Figure 2B), and at 942, 954, 960, 971, 981, and 992 cm^{-1} (Figures 2D and 3) in xanthorhodopsin. The fourth band at ~985 cm^{-1}, which we assign exclusively to K_E, is not expected to be strong and is not seen at 77K in Raman[36,94] but was observed, in accord with our expectations, at room temperature in nanosecond time-resolved CARS[32] and Raman[22] at 984 cm^{-1} and at 987 cm^{-1}, respectively. The last two bands at 963 and 997 cm^{-1} in bacteriorhodopsin and at 954 and 992 cm^{-1} in xanthorhodopsin are present in both K_0 and K_E states and exhibit no temperature dependence (Figure 4A). Thus, of the two most interesting bands (Figure 4), at ~960 cm^{-1} (at 956 cm^{-1} in bacteriorhodopsin and at 961 cm^{-1} in xanthorhodopsin), which we assigned exclusively to K (Figure 6A), and at ~980 cm^{-1} (at 985 cm^{-1} in bacteriorhodopsin and at 981 cm^{-1} in xanthorhodopsin), which we assigned exclusively to K (Figure 6A), the latter received no clear assignment. The former one, at ~960 cm^{-1}, is known to be[42] the one significantly affected by H_2O/D_2O exchange (see also Figure 1), and its assignment to the 15-HOOP mode (coupled through the double bond to the N-H/D HOOP) has never been challenged.

However, when an assignment was made for the band at ~980 cm^{-1} from FTIR data[24], it yielded a seemingly paradoxical conclusion that it also (as the band at ~960 cm^{-1}) belongs to the 15-HOOP mode. The HOOP band frequencies do not display significant temperature dependence. For example, the strongest band in low-temperature static spectra in bacteriorhodopsin is at 956 cm^{-1}[15,42], and at ~960 cm^{-1} in room-temperature picosecond spectra[32,39], and, therefore, the increasing amplitude at ~980 cm^{-1} in the trapped mixture at higher temperatures (Figure 4) can hardly be explain as an up-shift of its frequency (from ~960 to ~980 cm^{-1}) by temperature-induced factors. Thus, if the band at ~980 cm^{-1} reflects the same mode as the ~960 cm^{-1} band, i.e., 15-HOOP, its increasing amplitude has to be due to the increasing presence of a different intermediate in mixtures trapped at higher temperatures. Therefore, the simultaneous HOOP intensities at ~960 and ~980 cm^{-1} (in the whole 80-180K range in Figure 4) is direct evidence that the trapped states not only at 140 and 180K, but also at 77K are not pure states but are mixtures of K_0 and K_E, each contributing its own 15-HOOP mode, at ~960 cm^{-1} an at ~980 cm^{-1}, respectively.

Alternatively, the mode that gives rise to the increasing band at ~980 cm^{-1} at higher temperatures (Figure 3) is not from the 15-HOOP, but rather the vibration that contributes to the Raman band at 975 cm^{-1} (obtained with a 5 cm^{-1} resolution), which was assigned to the coupled 7,8-HOOP, i.e. wags of the C_7-H and the C_8-H (coupled in-phase $-HC_7=C_8H-$)[50]. If so, the evolution of the HOOP pattern upon heating between 80 and 140K in bacteriorhodopsin, and to ~180K in xanthorhodopsin provides an interesting possibility, as follows. In the K_0 state the $-C_7=C_8-$ bonds are virtually undisturbed (absence of a band at ~980 cm^{-1} in Figure 6) in contrast to the strongly distorted $=C_{14}-C_{15}=$ bonds (the intense band at ~960 cm in Figure 6), and the torsional distortion at this early stage is localized close to the Schiff base end of the polyene chain with little if any torsional distortions close to the ionone ring. This pattern is reversed upon the K_0-to-K_E transition (Figure 4), and in the K_E state the strongest distortion is in the $-C_7=C_8$-region, close to the ionone ring, while the $-C_{15}=N-$ region seems to be relaxed. This relaxation (although only partial, due to distributed kinetics) takes place in bacteriorhodopsin within minutes at temperatures as low as ~140K (~50% conversion) or even as low as ~80K (~20% conversion). The distortion in the $-C_7=C_8-$ region (the band at ~980 cm) relaxes later, in two stages during the K_E-to-K_L and the K_L-to-L transitions, observable at ambient temperature on the time-scale of ~100 ns[28] and 1.2 μs[28], respectively.

Both X-ray crystallography[95] and solid-state NMR [92] of the K state at cryogenic temperatures (predominantly K_0, see Figure 7) reveal major torsional distortions near the site of isomerization in the retinal. Thus, the structure of the retinal in K_0 represents a distorted 13-*cis* isomer, which relaxes into planar 13-*cis* isomer in L[96] during the K_0-to-K_E-to-K_L transitions, as witnessed by the HOOP band relaxation. It is not clear at this point which of the three steps, the K_0-to-K_E, the K_E-to-K_L or the K_L-to-L (in tens of picoseconds[38], in hundreds of nanoseconds[28] or in microseconds[28], respectively) is responsible for most of relaxation. In bacteriorhodopsin neither K_E nor K_L can be easily trapped for crystallographic structure determination due to interference from L, which begins to appear above ~140K[48]. The extended temperature range in xanthorhodopsin, in which the K-like states coexist without interference from L (Figure 2), makes it possible to study the K_0-to-K_E reaction in more detail.

Some residual HOOP bands (~15% intensity) could be found in time-resolved spectra of L as well[28,85], which allows alternative interpretations. On the one hand, it is possible that the HOOP intensities are characteristic not only for the K-like states but for the L state as well, and, therefore, the retinal is still somewhat twisted in L. The crystallographic data on L does not show sufficient torsional distortions[96], and the Raman spectra produce no prominent HOOP bands[50]. On the other hand, it is much more probable that the residual HOOP intensity is due to the incomplete deconvolution of the K_L and L kinetics when the back-reaction, $K_L \leftarrow L$[97-99], was not properly taken into account[28]. Then, the anomalously intense HOOP bands are a unique characteristic feature of the (red-shifted) intermediates, K-like[15,24,28,42] and O-like[61], formed immediately after isomerization, which have not yet had a chance to relax their torsion stress. We favor this latter interpretation.

Conclusions

Three K-like states, K_0, K_E and K_L, occur in a sequence in the photocycles of both bacteriorhodopsin and xanthorhodopsin. In IR these states are distinguished primarily in the HOOP (K_0 vs. K_E) and ethylenic (K_E vs. K_L)[28] regions. Contrarily to widely-held belief, trapping even at 77K does not result in a single intermediate. Rather the K_0 and K_E states co-exist in the temperature range from ~50 to ~230K as binary mixtures (plus the L state above 140K in bacteriorhodopsin and above 190K in xanthorhodopsin). When trapped at 77K the contribution of K_E is ~15% and ~10% in bacteriorhodopsin and xanthorhodopsin, respectively.

Interconversion of K_0-to-K_E is unidirectional, proceeding with a distributed kinetics that is characterized by a barrier-height distribution wider than the ~7 kJ/mol, measured previously for a later reaction, the L-formation[48].

Two different, rather than one[34], weakly-bound water molecules are disturbed in both proteins during the life-span of the K-like states: one in K_0, the other in K_E. In bacteriorhodopsin the first was assigned to water 401[34], the other might have been assigned to water 407. Unlike bacteriorhodopsin, xanthorhodopsin lacks these weakly-bound water molecules[67], presenting a challenge to the interpretation of the observed distortions of weakly-bound water molecules.

Acknowledgments

This work was supported in part by grants to J.K.L. from NIH (5R37GM029498), DOE (DEFG03-86ER13525), and Army Research Office (W911NF-09-1-0243). The authors are grateful to Drs. S.P. Balashov and E.S. Imasheva for valuable discussions and for partly purified preparations of xanthorhodopsin.

References

1. Béjà O, Spudich EN, Spudich JL, Leclerc M, DeLong EF. Nature. 2001; 411:786–789. [PubMed: 11459054]
2. Wang WW, Sineshchekov OA, Spudich EN, Spudich JL. J.Biol.Chem. 2003; 278:33985–33991. [PubMed: 12821661]
3. Sabehi G, Massana R, Bielawski JP, Rosenberg M, DeLong EF, Beja O. Environ.Microbiol. 2003; 5:842–849. [PubMed: 14510837]
4. Brown LS. Photochem.Photobiol.Sci. 2004; 3:555–565. [PubMed: 15170485]
5. Lanyi JK. Annu.Rev.Physiol. 2004; 66:665–688. [PubMed: 14977418]
6. Hoff WD, Jung KH, Spudich JL. Ann.Rev.Biophys.Biomol.Struc. 1997; 26:223–258.
7. Lozier RH, Bogomolni RA, Stoeckenius W. Biophys.J. 1975; 15:955–962. [PubMed: 1182271]
8. Dinur U, Honig B, Ottolenghi M. Photochem.Photobiol. 1981; 33:523–527.
9. Stoeckenius W, Lozier RH. J.Supramol.Struct. 1974; 2:769–774. [PubMed: 4461852]
10. Litvin FF, Balashov SP, Sineshchekov VA. Bioorgan.Khim. 1975; 1:1767–1777.
11. Applebury ML, Peters KS, Rentzepis PM. Biophys.J. 1978; 23:375–382. [PubMed: 698342]
12. Iwasa T, Tokunaga F, Yoshizawa T. FEBS Lett. 1979; 101:121–124. [PubMed: 446722]
13. Polland HJ, Franz MA, Kaiser W, Kölling E, Oesterhelt D, Zinth W. Biophys.J. 1986; 49:651–662. [PubMed: 19431670]
14. Shichida Y, Matuoka S, Hidaka Y, Yoshizawa T. Biochim.Biophys.Acta. 1983; 723:240–246.
15. Rothschild KJ, Roepe PD, Gillespie J. Biochim.Biophys.Acta. 1985; 808:140–148. [PubMed: 4005227]
16. Dioumaev AK, Lanyi JK. J.Phys.Chem.B. 2009 in press. [PubMed: 19994879]
17. Mao B. Photochem.Photobiol. 1981; 33:407–411.
18. Kalisky O, Ottolenghi M. Photochem.Photobiol. 1982; 35:109–115.
19. Balashov SP, Karneeva NV, Litvin FF. Biologicheskie Membrany. 1990; 7:586–592.
20. Balashov SP, Karneyeva NV, Litvin FF, Ebrey TG. Photochem.Photobiol. 1991; 54:949–953.
21. Kuschmitz D, Hess B. FEBS Lett. 1982; 138:137–140.
22. Braiman MS. Methods in Enzymology. 1986; 127:587–597.
23. Diller R, Iannone M, Cowen BR, Maiti S, Bogomolni RA, Hochstrasser RM. Biochemistry. 1992; 31:5567–5572. [PubMed: 1610802]
24. Weidlich O, Siebert F. Appl.Spectrosc. 1993; 47:1394–1400.
25. Sasaki J, Maeda A, Kato C, Hamaguchi H. Biochemistry. 1993; 32:867–871. [PubMed: 8422391]
26. Sasaki J, Yuzawa T, Kandori H, Maeda A, Hamaguchi H. Biophys.J. 1995; 68:2073–2080. [PubMed: 7612850]
27. Hage W, Kim M, Frei H, Mathies RA. J.Phys.Chem. 1996; 100:16026–16033.
28. Dioumaev AK, Braiman MS. J.Phys.Chem.B. 1997; 101:1655–1662.
29. Hsieh C-L, Nagumo N, Nicol M, El-Sayed MA. J.Phys.Chem. 1981; 85:2714–2717.
30. Hsieh C-L, El-Sayed MA, Nicol M, Nagumo M, Lee J-H. Photochem.Photobiol. 1983; 38:83–94.
31. Mizuno M, Shibata M, Yamada J, Kandori H, Mizutani Y. J.Phys.Chem.B. 2009; 113:12121–12128. [PubMed: 19678662]
32. Weidlich O, Ujj L, Jager F, Atkinson GH. Biophys.J. 1997; 72:2329–2341. [PubMed: 9129836]
33. Dioumaev AK, Keszthelyi L. Acta Biochimica et Biophysica Hungarica. 1988; 23:271–278. [PubMed: 3150196]
34. Maeda A, Verhoeven MA, Lugtenburg J, Gennis RB, Balashov SP, Ebrey TG. J.Phys.Chem.B. 2004; 108:1096–1101.
35. Braiman MS, Mathies RA. Proc.Natl.Acad.Sci.U.S.A. 1982; 79:403–407. [PubMed: 6281770]
36. Smith, SO.; Braiman, MS.; Mathies, RA. Time-resolved vibrational spectroscopy. Academic Press; N.Y.: 1983. p. 219-230.
37. Brack TL, Atkinson GH. J.Mol.Struct. 1989; 214:289–303.
38. Doig SJ, Reid PJ, Mathies RA. J.Phys.Chem. 1991; 95:6372–6379.

39. Shim S, Dasgupta J, Mathies RA. J.Am.Chem.Soc. 2009; 131:7592–7597. [PubMed: 19441850]
40. Terentis AC, Ujj L, Abramczyk H, Atkinson GH. Chem.Phys. 2005; 313:51–62.
41. Rothschild KJ, Marrero H. Proc.Natl.Acad.Sci.U.S.A. 1982; 79:4045–4049. [PubMed: 6955790]
42. Bagley K, Dollinger G, Eisenstein L, Singh AK, Zimányi L. Proc.Natl.Acad.Sci.U.S.A. 1982; 79:4972–4976. [PubMed: 6956906]
43. Siebert F, Mäntele W. Eur.J.Biochem. 1983; 130:565–573. [PubMed: 6825710]
44. Gerwert K, Siebert F. EMBO J. 1986; 5:805–811. [PubMed: 16453681]
45. Diller R, Maiti S, Walker GC, Cowen BR, Pippenger RS, Bogomolni RA, Hochstrasser RM. Chem.Phys.Lett. 1995; 241:109–115.
46. Maeda A, Sasaki J, Pfefferlé J-M, Shichida Y, Yoshizawa T. Photochem.Photobiol. 1991; 54:911–921.
47. Kandori H. Biochim.Biophys.Acta. 2000; 1460:177–191. [PubMed: 10984599]
48. Dioumaev AK, Lanyi JK. Proc.Natl.Acad.Sci.U.S.A. 2007; 104:9621–9626. [PubMed: 17535910]
49. Smith SO, Lugtenburg J, Mathies RA. J.Mem.Biol. 1985; 85:95–109.
50. Smith, SO. Ph.D. thesis. University of California; Berkeley: 1985. Resonance Raman studies on the mechanism of proton translocation by bacteriorhodopsin's retianl chromophore.
51. Rothschild KJ, Roepe PD, Lugtenburg J, Pardoen JA. Biochemistry. 1984; 23:6103–6109. [PubMed: 6525348]
52. Dioumaev AK, Braiman MS. Photochem.Photobiol. 1997; 66:755–763. [PubMed: 9421962]
53. Kandori H, Shimono K, Sudo Y, Iwamoto M, Shichida Y, Kamo N. Biochemistry. 2001; 40:9238–9246. [PubMed: 11478891]
54. Shimono K, Furutani Y, Kandori H, Kamo N. Biochemistry. 2002; 41:6504–6509. [PubMed: 12009914]
55. Bergo V, Amsden JJ, Spudich EN, Spudich JL, Rothschild KJ. Biochemistry. 2004; 43:9075–9083. [PubMed: 15248764]
56. Furutani Y, Bezerra AG Jr. Waschuk S, Sumii M, Brown LS, Kandori H. Biochemistry. 2004; 43:9636–9646. [PubMed: 15274618]
57. Furutani Y, Kawanabe A, Jung KH, Kandori H. Biochemistry. 2005; 44:12287–12296. [PubMed: 16156642]
58. Furutani Y, Sumii M, Fan Y, Shi LC, Waschuk SA, Brown LS, Kandori H. Biochemistry. 2006; 45:15349–15358. [PubMed: 17176057]
59. Furutani Y, Sudo Y, Wada A, Ito M, Shimono K, Kamo N, Kandori H. Biochemistry. 2006; 45:11836–11843. [PubMed: 17002284]
60. Ikeda D, Furutani Y, Kandori H. Biochemistry. 2007; 46:5365–5373. [PubMed: 17428036]
61. Smith SO, Pardoen JA, Lugtenburg J, Curry B, Mathies RA. Biochemistry. 1983; 22:6141–6148.
62. Maeda A. Israel J.Chem. 1995; 35:387–400.
63. Suzuki D, Sudo Y, Furutani Y, Takahashi H, Homma M, Kandori H. Biochemistry. 2008; 47:12750–12759. [PubMed: 18991393]
64. Balashov SP, Imasheva ES, Boichenko VA, Anton J, Wang JM, Lanyi JK. Science. 2005; 309:2061–2064. [PubMed: 16179480]
65. Dioumaev AK, Lanyi JK. Biochemistry. 2008; 47:11125–11133. [PubMed: 18821776]
66. Oesterhelt D, Stoeckenius W. Methods in Enzymology. 1974; 31:667–678. [PubMed: 4418026]
67. Luecke H, Schobert B, Stagno J, Imasheva ES, Wang JM, Balashov SP, Lanyi JK. Proc.Natl.Acad.Sci.U.S.A. 2008; 105:16561–16565. [PubMed: 18922772]
68. Dioumaev AK, Lanyi JK. Photochem.Photobiol. 2009; 85:598–608. [PubMed: 19192202]
69. Golub, GH.; Van Loan, CF. Matrix computations. Johns Hopkins University Press; Baltimore: 1996. p. 1-694.
70. Korenstein R, Hess B. FEBS Lett. 1977; 82:7–11. [PubMed: 913579]
71. Roepe PD, Ahl PL, Herzfeld J, Lugtenburg J, Rothschild KJ. J.Biol.Chem. 1988; 263:5110–5117. [PubMed: 3356682]

72. Mizuide N, Shibata M, Friedman N, Sheves M, Belenky M, Herzfeld J, Kandori H. Biochemistry. 2006; 45:10674–10681. [PubMed: 16939219]
73. Earnest TN, Roepe PD, Braiman MS, Gillespie J, Rothschild KJ. Biochemistry. 1986; 25:7793–7798. [PubMed: 3801443]
74. Kandori H, Kinoshita N, Shichida Y, Maeda A. J.Phys.Chem.B. 1998; 102:7899–7905.
75. Dioumaev AK. Biochemistry (Moscow). 2001; 66:1269–1276.
76. Sonar S, Marti T, Rath P, Fischer W, Coleman M, Nilsson A, Khorana HG, Rothschild KJ. J.Biol.Chem. 1994; 269:28851–28858. [PubMed: 7961844]
77. Barth A. Biochim.Biophys.Acta. 2007; 1767:1073–1101. [PubMed: 17692815]
78. Fischer WB, Sonar S, Marti T, Khorana HG, Rothschild KJ. Biochemistry. 1994; 33:12757–12762. [PubMed: 7947680]
79. Maeda A, Sasaki J, Ohkita YJ, Simpson M, Herzfeld J. Biochemistry. 1992; 31:12543–12545. [PubMed: 1472491]
80. Luecke H, Schobert B, Richter H-T, Cartailler JP, Lanyi JK. J.Mol.Biol. 1999; 291:899–911. [PubMed: 10452895]
81. Bellamy, LJ. The infra-red spectra of complex molecules. 3rd ed.. Chapman and Hall - Wiley; London & New York: 1975. p. 1-433.
82. Aton B, Doukas AG, Callender RH, Becher B, Ebrey TG. Biochemistry. 1977; 16:2995–2999. [PubMed: 880292]
83. Xie AH, Nagle JF, Lozier RH. Biophys.J. 1987; 51:627–635. [PubMed: 3580488]
84. Hessling B, Souvignier G, Gerwert K. Biophys.J. 1993; 65:1929–1941. [PubMed: 8298022]
85. Rödig C, Chizhov I, Weidlich O, Siebert F. Biophys.J. 1999; 76:2687–2701. [PubMed: 10233083]
86. Dioumaev AK. Biophys.Chem. 1997; 67:1–25. [PubMed: 17029887]
87. Nuss MC, Zinth W, Kaiser W, Kolling E, Oesterhelt D. Chem.Phys.Lett. 1985; 117:1–7.
88. Sharkov AV, Pakulev AV, Chekalin SV, Matveetz YA. Biochim.Biophys.Acta. 1985; 808:94–102.
89. Kaminaka S, Mathies RA. Laser Chemistry. 1999; 19:165–168.
90. Eyring G, Curry B, Broek A, Lugtenburg J, Mathies R. Biochemistry. 1982; 21:384–393. [PubMed: 7074022]
91. Eyring G, Curry B, Mathies R, Fransen R, Palings I, Lugtenburg J. Biochemistry. 1980; 19:2410–2418. [PubMed: 7387982]
92. Mak-Jurkauskas ML, Bajaj VS, Hornstein MK, Belenky M, Griffin RG, Herzfeld J. Proc.Natl.Acad.Sci.U.S.A. 2008; 105:883–888. [PubMed: 18195364]
93. Koyama, Y. Carotenoids. Birkhaeuser Verlag; Basel: 1995. p. 135-146.Chapter 5
94. Smith SO, Myers AB, Mathies RA, Pardoen JA, Winkel C, van den Berg EMM, Lugtenburg J. Biophys.J. 1985; 47:653–664. [PubMed: 4016185]
95. Schobert B, Cupp-Vickery J, Hornak V, Smith SO, Lanyi JK. J.Mol.Biol. 2002; 321:715–726. [PubMed: 12206785]
96. Lanyi JK, Schobert B. J.Mol.Biol. 2007; 365:1379–1392. [PubMed: 17141271]
97. Zimányi L, Keszthelyi L, Lanyi JK. Biochemistry. 1989; 28:5165–5172. [PubMed: 2765529]
98. Zimányi L, Lanyi JK. Biophys.J. 1993; 64:240–251. [PubMed: 8431544]
99. Zimányi L, Saltiel J, Brown LS, Lanyi JK. J.Phys.Chem.A. 2006; 110:2318–2321. [PubMed: 16480288]

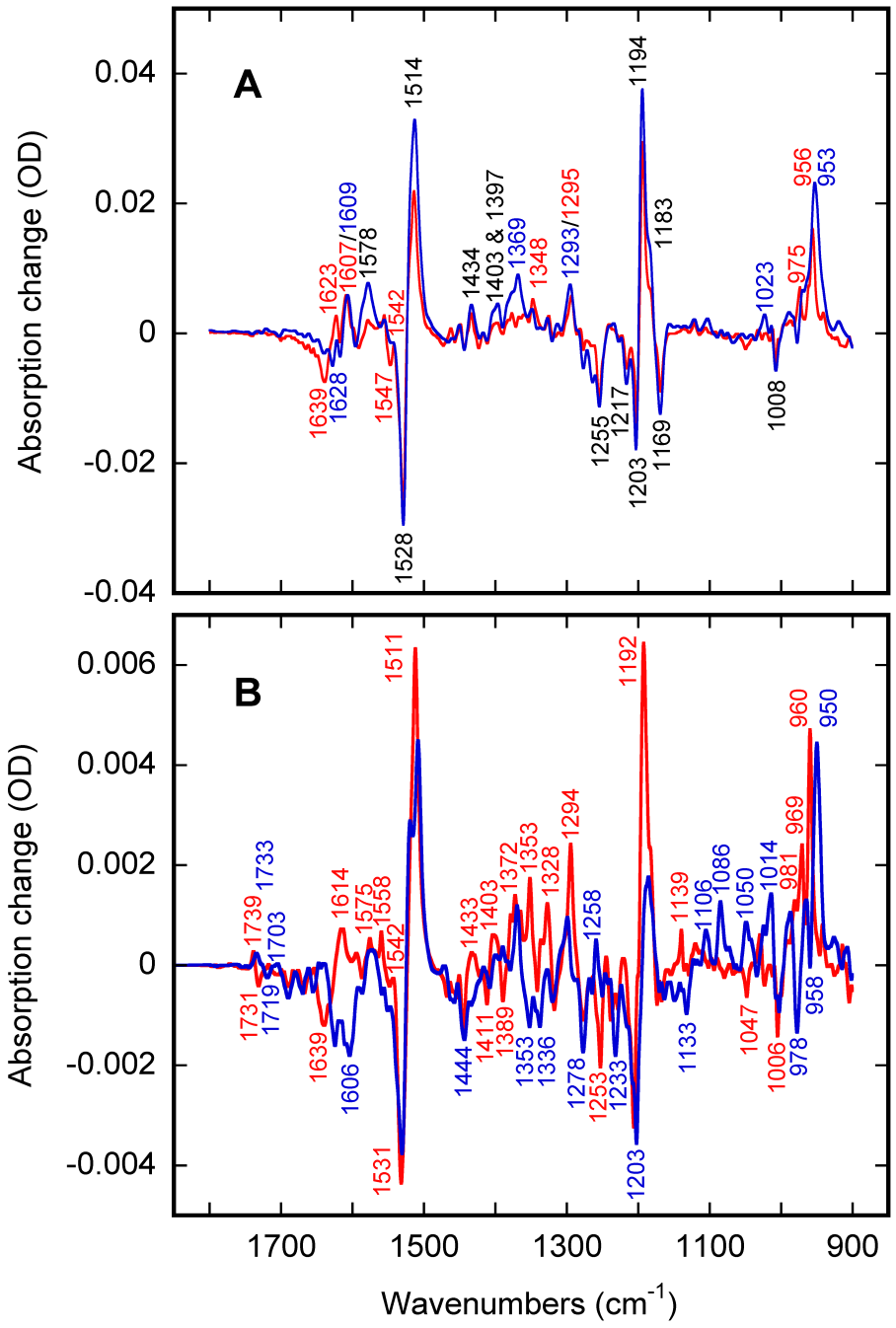

Figure 1.
Low-temperature FTIR spectra of bacteriorhodopsin (panel A) and xanthorhodopsin (panel B) in H_2O (red) and D_2O (blue), trapped during blue illumination at 80K.

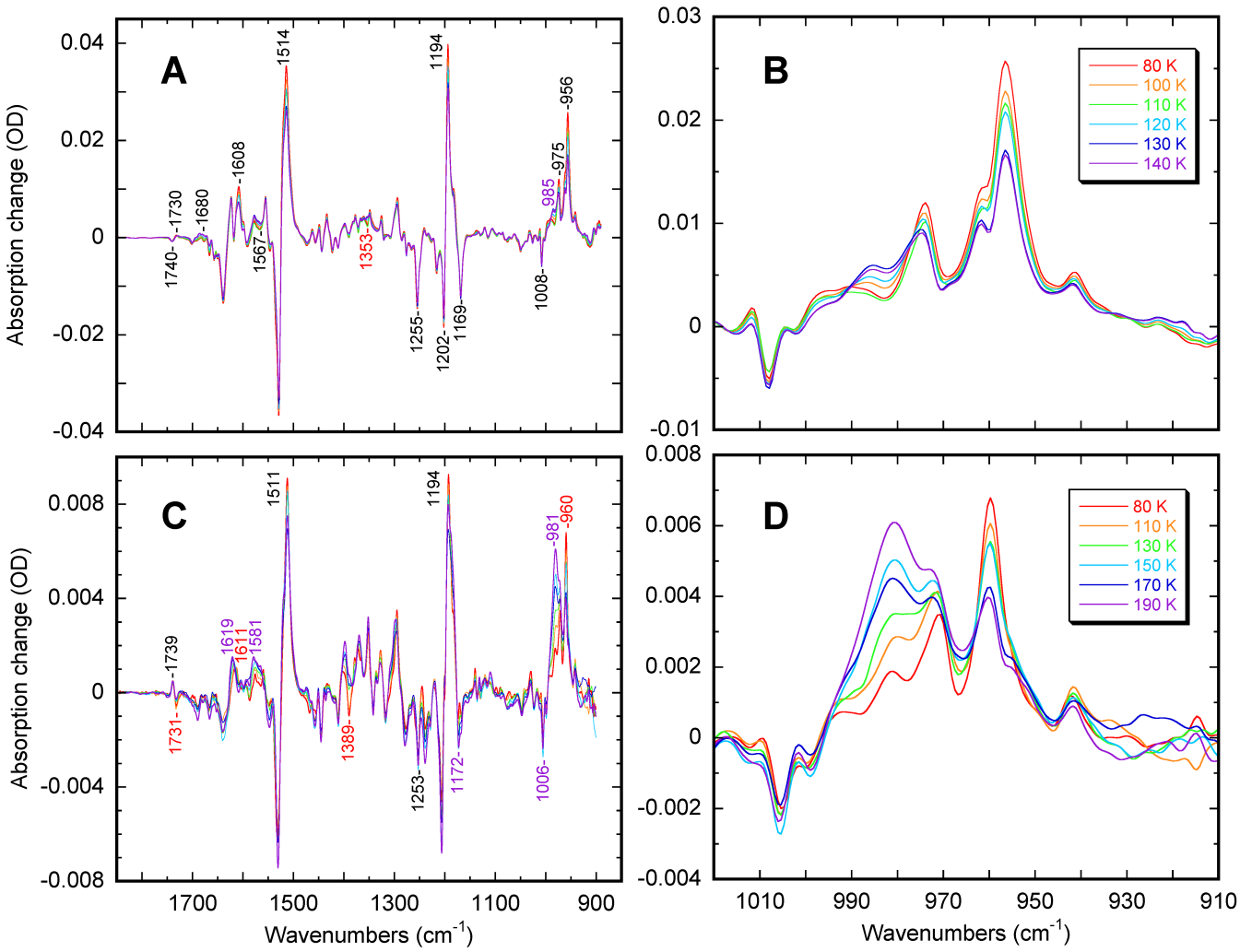

Figure 2.

Light-induced mixtures of K states trapped during blue-illumination at different temperatures. In bacteriorhodopsin (panels A and B) and in xanthorhodopsin (panels C and D) at 80K (red), 100K (yellow), 110K (green), 120K (cyan), 130K (blue) and 140K (magenta) for bacteriorhodopsin and at 80K (red), 110K (yellow), 130K (green), 150K (cyan), 170K (blue) and 190K (magenta) for xanthorhodopsin, respectively.

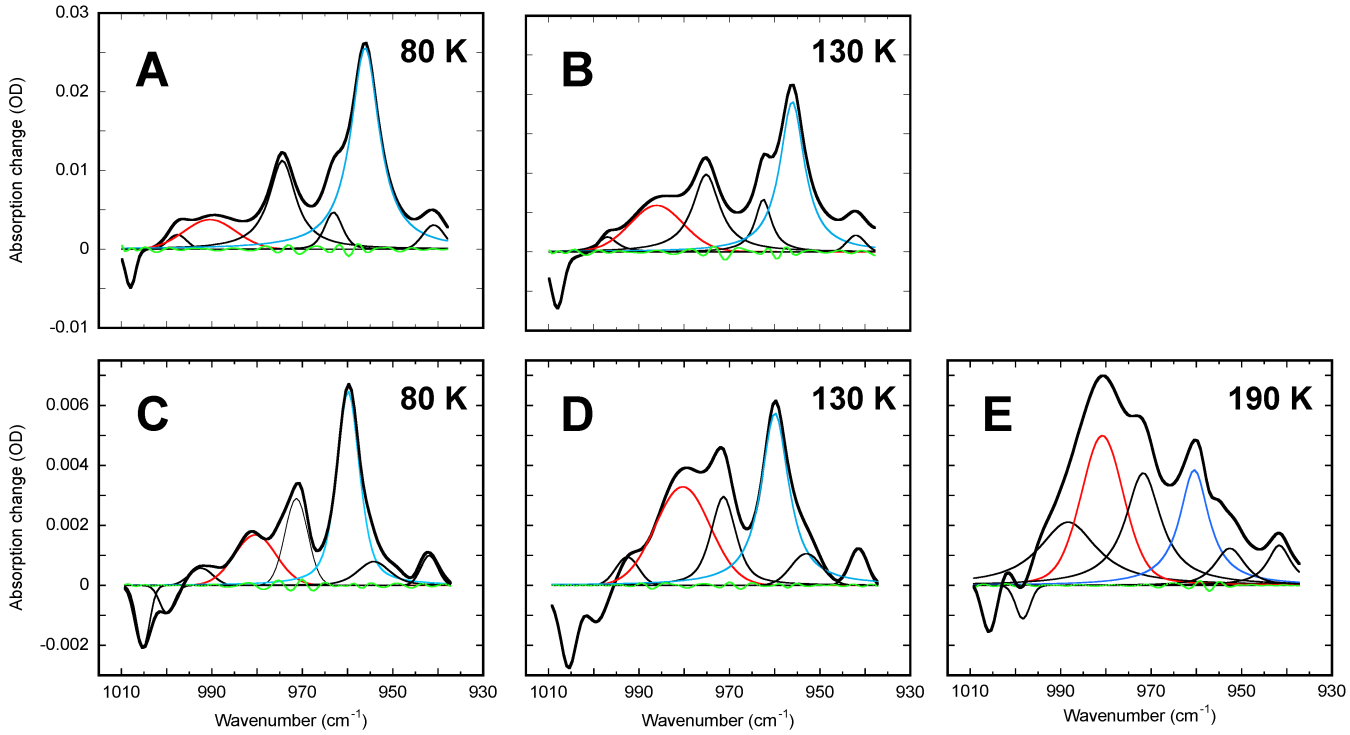

Figure 3.

Decomposition of the region of the HOOP bands (from Figure 2) with a weighted sum of Gaussian and Lorentzian components: in bacteriorhodopsin spectra at 80 and 130K (panel A and B), and in xanthorhodopsin spectra at 80, 130 and 190K (panel C-E). The deconvolution was done in GRAMS software, yielding fits with r^2 better than 0.997. The fit residuals are plotted in green. In bacteriorhodopsin the positions (their widths in brackets) for the fitted bands averaged over six temperatures are at: 941.6±0.4 cm^{-1} (5.1±0.6), 956.2±0.1 cm^{-1} (6.9±0.5), 962.9±0.4 cm^{-1} (5±1), 974.8±0.3 cm^{-1} (6.6±0.6), 985±2 cm^{-1} (15±1), 997.0±0.3 cm^{-1} (4.7±0.5), 1008.0±0.1 cm^{-1} (2.8±0.3). In xanthorhodopsin the corresponding values are: 941.5±0.3 cm^{-1} (5.2±0.7), 953.4±0.6 cm^{-1} (7.5±0.8), 960.0±0.2 cm^{-1} (6.8±0.6), 971.5±0.2 cm^{-1} (8±2), 980.5±0.6 cm^{-1} (12±1), 992±2 cm^{-1} (8±2), 999.0±0.7 cm^{-1} (5±1), 1005.6±0.2 cm^{-1} (4.1±0.3). The two main temperature-sensitive bands are at 956 cm^{-1} (in blue) and 985 cm^{-1} (in red) in bacteriorhodopsin (panel A-B), and at 960 cm^{-1} (in blue) and 981 cm^{-1} (in red) in xanthorhodopsin (panel C-E). Previously, the Raman band at 1008 cm^{-1} in non-excited BR_{568} was assigned to the symmetric methyl rock, i.e., to the in-plane rather than out-of-plane vibration[50], implying a similar assignment for the negative band (i.e. depletion in non-excited state) at 1008 cm^{-1} in bacteriorhodopsin and two similar bands, at ~1000 and at ~1005 cm^{-1}, in xanthorhodopsin.

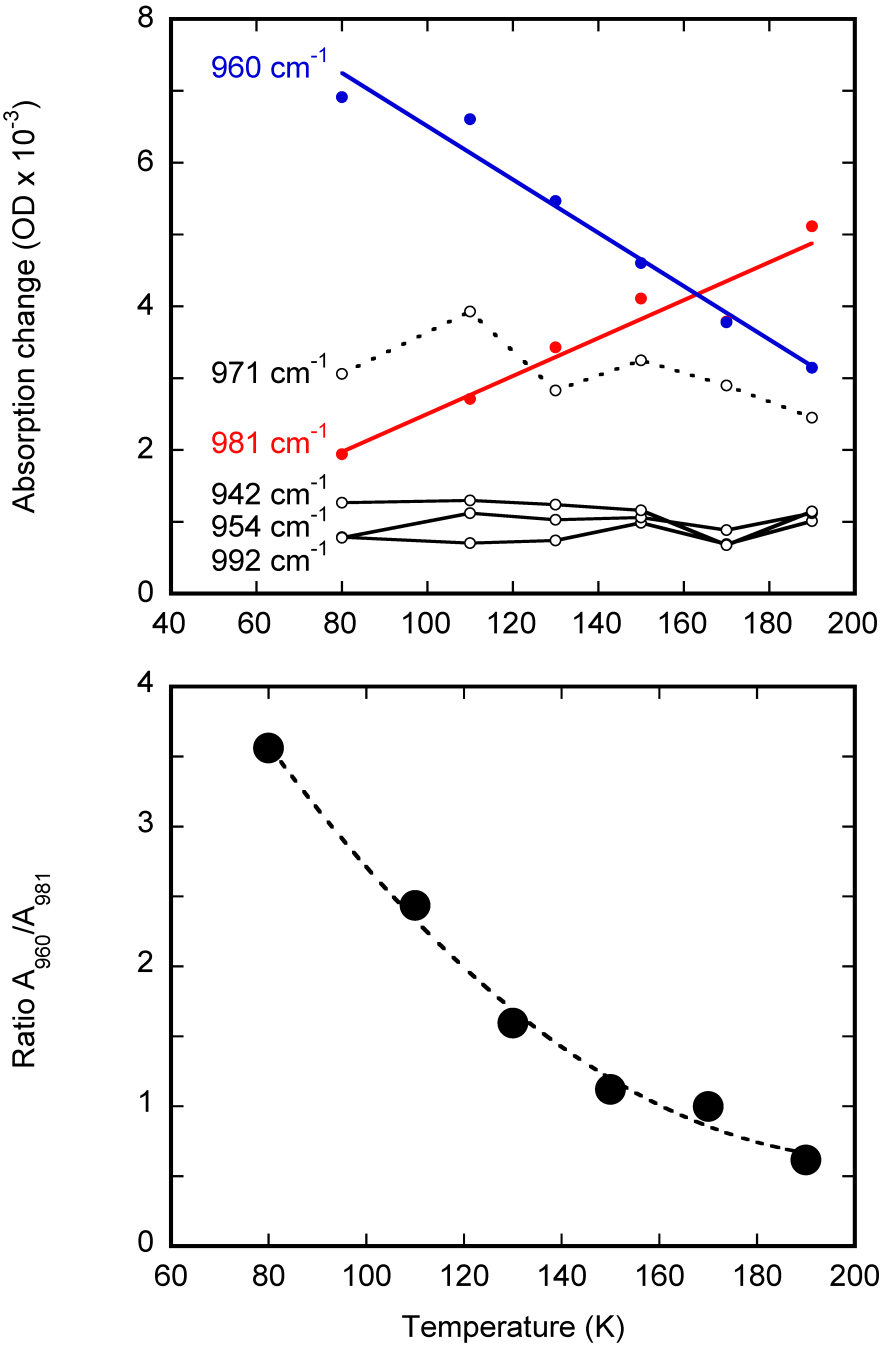

Figure 4.
Temperature dependence of the HOOP bands in xanthorhodopsin. Panel A: The amplitude of the decomposed components (as in Figure 3). Panel B: the ratio of amplitudes of the two main temperature-dependent bands A_{960}/A_{981}.

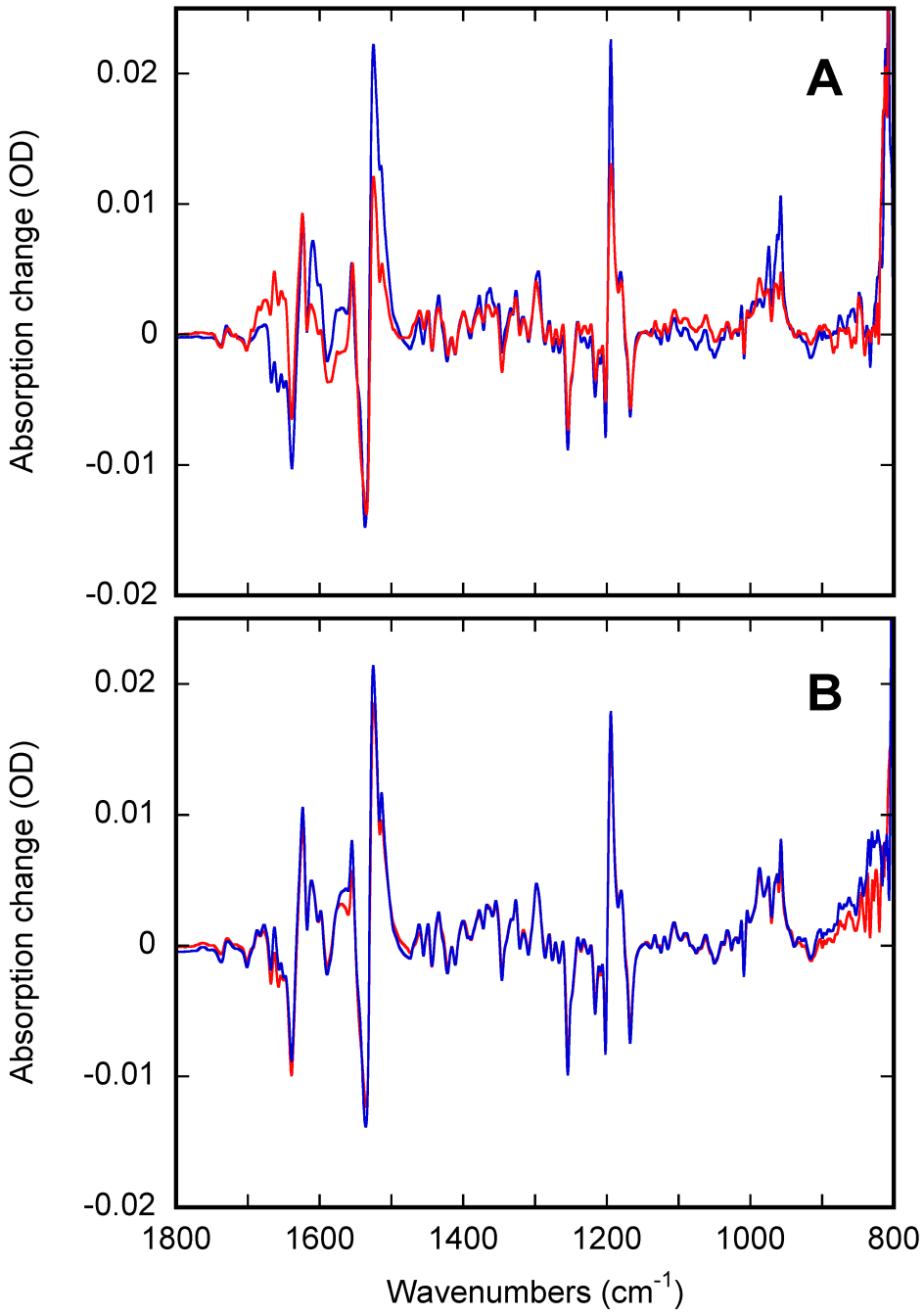

Figure 5.
Temperature perturbation experiments with bacteriorhodopsin. Panel A: Effect of up-shift of temperature, which illustrates the forward reaction; the light-induced conversion was initiated at 80K (in blue) and the sample was later heated to 140K (in red) in the dark. Panel B: Absence of effect from down-shift of temperature, which illustrates the absence of the back reaction; the light-induced conversion was initiated at 140K (in red) and the sample was later cooled to 80K (in red) in the dark. The shoulder in the ethylenic band reflects incomplete light-adaptation, most probably due to insufficient hydration of the sample.

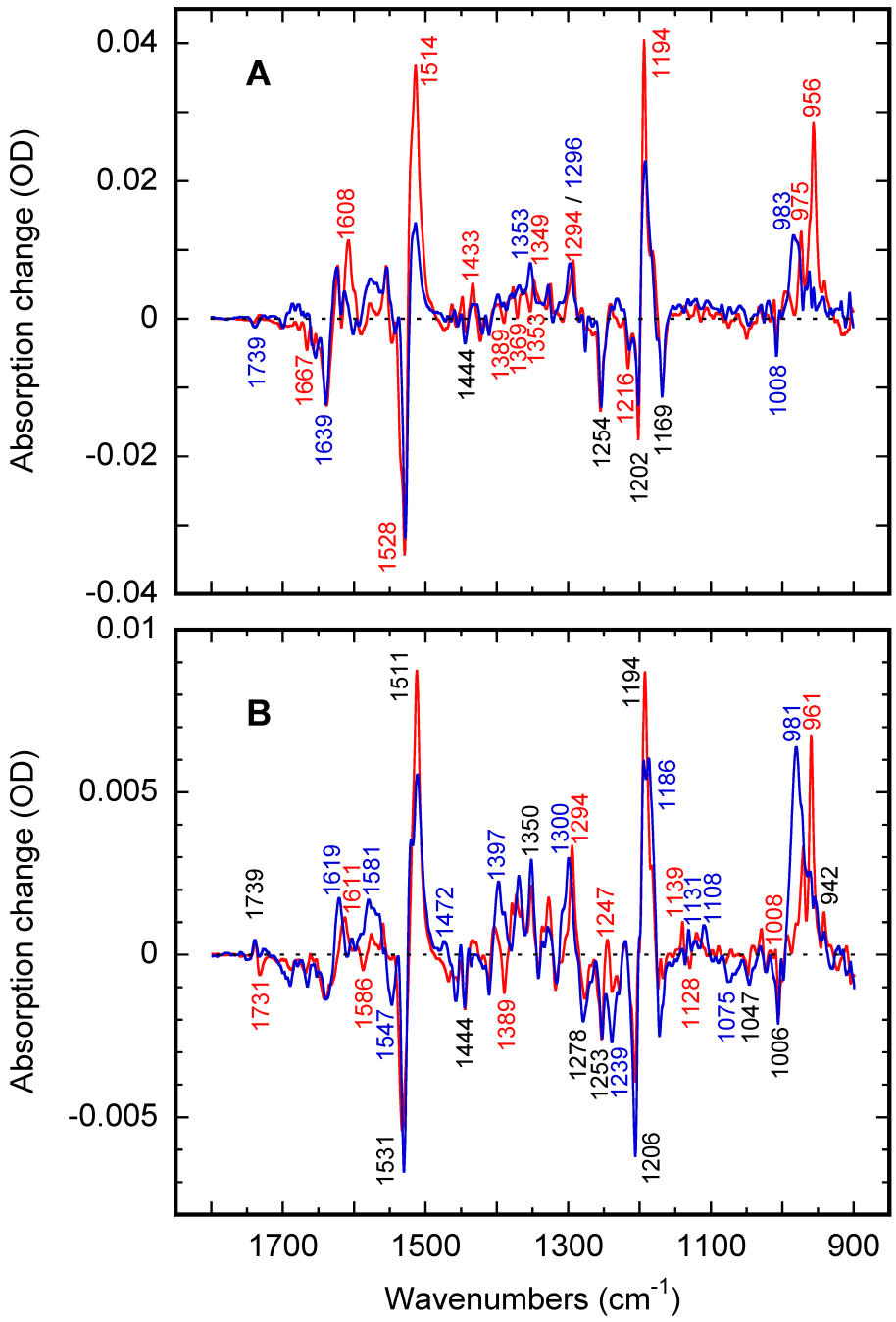

Figure 6.
Two distinct K intermediates in bacteriorhodopsin (panel A) and xanthorhodopsin (panel B) obtained from the spectra in Figure 2 by decomposition, involving SVD, rotation, and subtraction (see text for details).

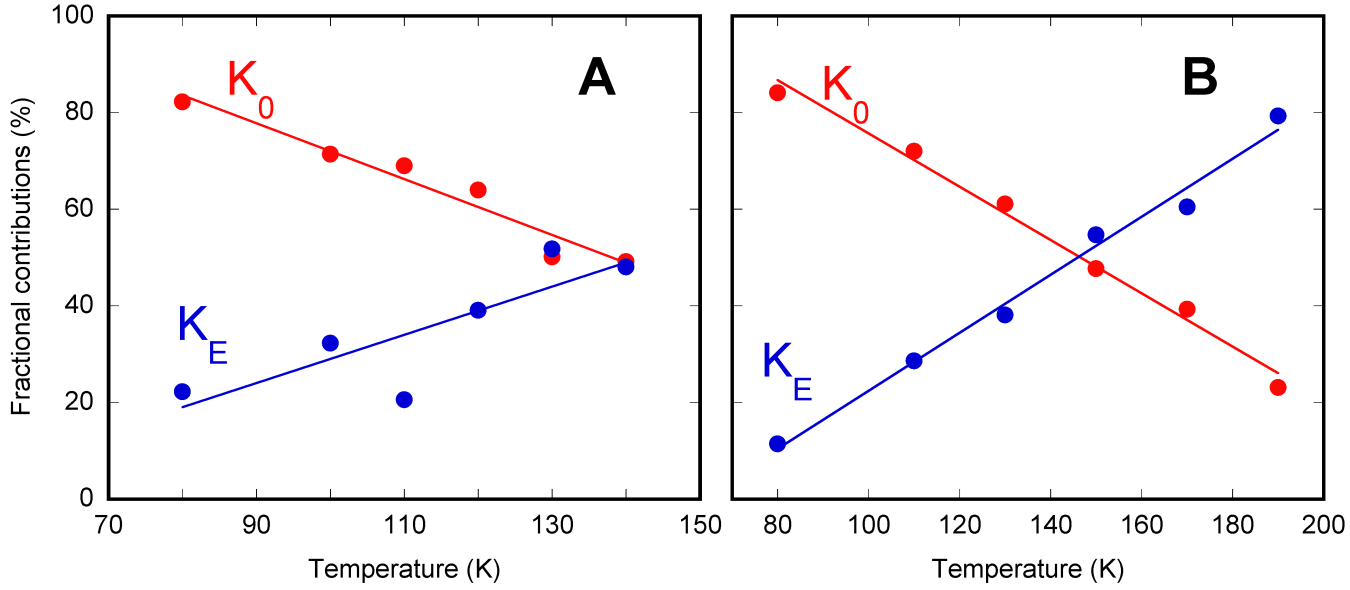

Figure 7.
Fractional contributions for the two K states calculated using the deconvoluted spectra of the pure forms (Figure 6) and the raw spectra in Figure 2 (see text for details).

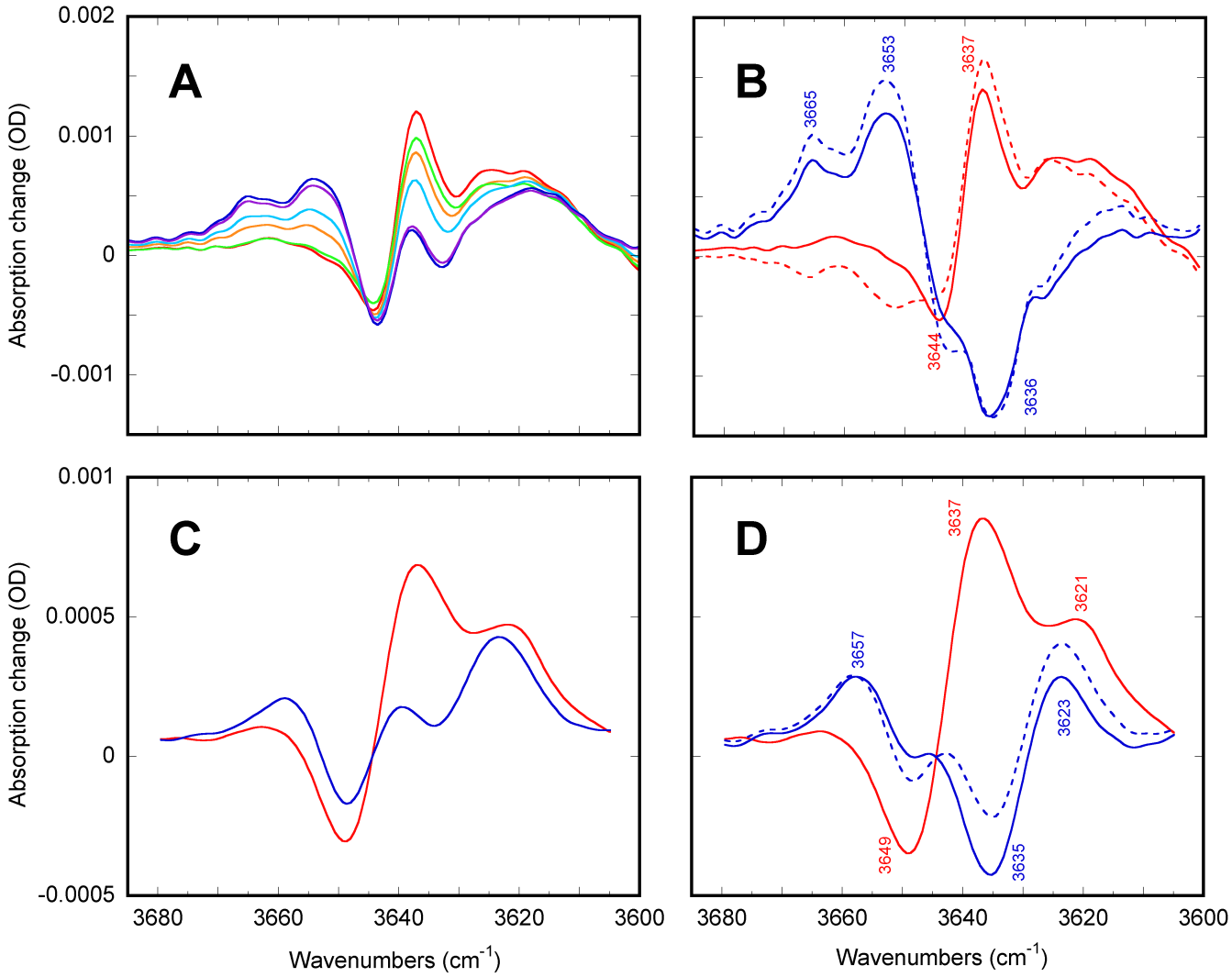

Figure 8.

The spectra of the two K-like states in the water region in bacteriorhodopsin (panel A and B) and in xanthorhodopsin (panel C and D). The spectra in panels A and B are at 2 cm^{-1}, as all the rest data in this paper; for presentation purposes the spectra in panels C and D were additionally smoothed to ~3.5 cm^{-1} resolution. Panels A and C are the measured IR spectra (corresponding to the spectra in Figure 2) of mixtures of the two K-like states trapped during blue light illumination at particular temperatures. Panel A: in bacteriorhodopsin at 80 (red), 100 (yellow), 110 (green), 120 (cyan), 130 (blue) and 140K (magenta). Panel B: in xanthorhodopsin at 85K (red) and 180K (blue). Panel B and D: Spectral decomposition based on the relative contributions (Figure 7) of the two states calculated from spectra in Figure 6 (dashed lines) and their additional adjustment (solid lines). See text for details.